



Published in final edited form as:

Pediatr Res. 2020 June ; 87(7): 1185–1192. doi:10.1038/s41390-019-0684-1.

Nephron loss detected by MRI following neonatal acute kidney injury in rabbits

Jennifer R Charlton^{1,*}, Edwin J Baldelomar², Kimberly deRonde¹, Helen P Cathro³, Nathan P Charlton⁴, Stacey Criswell⁵, Dylan Hyatt⁶, Sejin Nam⁷, Valeria Pearl¹, Kevin M Bennett⁸

¹University of Virginia, School of Medicine, Department of Pediatrics, Division of Nephrology, Charlottesville, VA

²Washington University in St. Louis, St. Louis, MI

³University of Virginia, School of Medicine, Department of Pathology, Charlottesville, VA

⁴University of Virginia, School of Medicine, Department of Emergency Medicine, Division of Medical Toxicology, Charlottesville, VA

⁵University of Virginia, School of Medicine, Department of Cell Biology, Charlottesville, VA

⁶University of Virginia, School of Medicine, Charlottesville, VA

⁷University of Hawaii, Department of Physics, Honolulu, HI

⁸Mallinckrodt Institute of Radiology, St. Louis, MI

Abstract

Background: Acute kidney injury affects nearly 30% of preterm neonates in the intensive care unit. We aimed to determine if nephrotoxin-induced AKI disrupted renal development assessed by imaging (CFE-MRI).

Methods: Neonatal New Zealand rabbits received indomethacin and gentamicin (AKI) or saline (control) for four days followed by cationic ferritin (CF) at six weeks. *Ex vivo* images were acquired using a gradient echo pulse sequence on 7T MRI. Glomerular number (N_{glom}) and apparent glomerular volume (aV_{glom}) were determined. CF toxicity was assessed at 2 and 28 days in healthy rabbits.

Results: N_{glom} was lower in the AKI group as compared to controls (74,034 vs 198,722, $p < 0.01$). aV_{glom} was not different (AKI: 7.3×10^{-4} vs. control: 6.2×10^{-4} mm³, $p = 0.69$). AKI kidneys had a band of glomeruli distributed radially in the cortex that were undetectable by MRI. Following CF injection, there was no difference in body or organ weights except for the liver, and transient changes in serum iron, platelets and white blood cell count.

Users may view, print, copy, and download text and data-mine the content in such documents, for the purposes of academic research, subject always to the full Conditions of use: http://www.nature.com/authors/editorial_policies/license.html#terms

***Corresponding author:** Jennifer R. Charlton, University of Virginia, Department of Pediatrics, Division of Nephrology, Box 800386, Charlottesville, VA 22903, phone: 434-924-2096, fax: 434-924-5505, jrc6n@virginia.edu.

Author contribution: JRC and KMB: designed the study and drafted and revised the paper; JRC, EJB, KdR, SC, DH, SN, VP: carried out experiments; JRC, EJB, HC, NPC, KMB: analyzed the data; and all authors approved the final version of the manuscript.

Disclosure statement: JRC and KMB are co-owners of Sindri Technologies, LLC

Conclusions: Brief nephrotoxin exposure during nephrogenesis results in fewer glomeruli and glomerular maldevelopment in a unique pattern detectable by MRI. Whole kidney evaluation by CFE-MRI may provide an important tool to understand the development of CKD following AKI.

INTRODUCTION:

Nearly 60% of nephrogenesis occurs in the third trimester of pregnancy (1), leaving a neonate born preterm to develop a majority of their lifetime supply of nephrons in an *ex utero* environment. Preterm neonates are exposed to a myriad of insults that can result in acute kidney injury (AKI), include postnatal hemodynamic changes, nephrotoxic burden (2) and comorbid maternal and neonatal conditions. AKI affects 48% of preterm neonates less than 29 weeks in the neonatal intensive care unit (3). Autopsy studies suggest preterm neonates have a shortened window for nephrogenesis (4) and those with AKI develop fewer nephrons (5) contributing to their risk for chronic kidney disease (CKD) (6, 7). However, despite the concern that AKI can contribute to the development of CKD, our current methods to categorize AKI and subsequent CKD are based on changes in serum creatinine which cannot detect permanent or subtle structural changes within the kidney (8, 9). In the neonatal population, in particular, nephron endowment would be a useful tool to assess the impact of AKI and stratify risk for CKD. However, it is not currently possible to quantify the microstructure of the whole human kidney *in vivo*; the number of glomeruli and their size can only be estimated from a renal biopsy and imaging (10) or determined postmortem (11). Recently, advancements have been made to measure nephron number *in vivo* in rat and mouse models (12, 13).

Contrast-enhanced MRI techniques have been developed to image renal microstructure (12, 14-18). Cationic ferritin (CF) has been used as a nanometer-sized, natural MRI contrast agent to noninvasively measure the number (N_{glom}) and apparent size (aV_{glom}) of each perfused glomerulus in mice (13, 14), rats (12, 16, 17), and human kidneys (15), both *ex vivo* and *in vivo*. CF injected intravenously into the live animal or into the renal artery of an excised kidney binds electrostatically to the anionic glomerular basement membrane (GBM). The iron core of ferritin makes the glomerulus MRI-visible. Cationic ferritin enhanced-MRI (CFE-MRI) enables novel investigations of spatial relationships between glomeruli, size distributions of glomeruli, and relationships of glomerular number, size and density to other structures such as the vasculature. CFE-MRI has the potential to reveal the number and size of glomeruli after neonatal AKI and may elucidate how CKD subsequently develops.

We employed a rabbit model neonatal AKI because glomerulogenesis naturally continues for 10 days after birth (19), providing a model of postnatal human nephrogenesis as in preterm neonates. Gentamicin and indomethacin were administered to reproduce the iatrogenic nephrotoxins routinely administered to many preterm neonates (2), and to determine if AKI affects glomerular microstructure (N_{glom} and aV_{glom}) during nephrogenesis in rabbits. We further investigated whether the contrast agent CF caused adverse effects in healthy juveniles. We hypothesized that N_{glom} , measured by CFE-MRI, would be lower after AKI and aV_{glom} would increase to maintain whole kidney glomerular filtration rate (GFR).

MATERIALS and METHODS:

Animal Preparation:

Animal experiments were approved by the University of Virginia Institutional Animal Care and Use Committee and were performed in accordance with the NIH Guide for the Care and Use of Laboratory Animals. Adult New Zealand rabbits were purchased from Robinson Services Incorporated (Mocksville, NC) and Charles River (Wilmington, MA) and bred at the University of Virginia. Juvenile offspring were used for all experiments. The study design is included in supplemental Figure S1.

AKI studies:

AKI was induced with indomethacin and gentamicin during the first week, an active period of nephrogenesis in rabbits. The drugs selected are commonly used in combination to treat sepsis in preterm neonates and often are associated with AKI in neonates (2). These drugs have been shown to cause AKI with reduced creatinine clearance when given to adult male rats (20). Here, kits in the AKI group (n=5) received indomethacin (5 mg/kg, oral; AvKARE, Inc. Pulaski, TN) and gentamicin (100 mg/kg, intraperitoneal injection, APP Pharmaceuticals, LLC; Schaumburg, IL) for four consecutive days beginning one week after birth (during the ten postnatal days of nephrogenesis). The control group received saline (n=5). Blood was collected for creatinine assessment at the age of three weeks to avoid the chance of maternal neglect. However, to confirm evidence of AKI, a kit from each group was euthanized at the completion of the four days of indomethacin and gentamicin. The kidneys from the AKI and control kits were fixed in formalin (10%) and embedded in paraffin. Tissues were sectioned at a thickness of 4 μ m. The sections were stained with period acid-Schiff and lotus lectin to identify kidney injury and assessed at 10x on an Olympus BX40 system microscope and QImaging Micropublisher 3.3 digital camera.

MRI Labeling Studies:

At six weeks, urine was collected from the kits from the AKI and control groups. They were sedated with isoflurane and an intravenous catheter was placed in the marginal ear vein. Hydrocortisone sodium succinate (10 mg/kg, intramuscular (IM) injection) was administered to each kit because CF is a horse-based product, as previously published (21). CF was prepared from native horse spleen ferritin (Sigma-Aldrich, St. Louis, MO) as described by Danon (22). Protein concentration of the CF was determined by Bradford assay. CF was administered to the AKI and control groups (1.92 mg/100 grams body weight infused over 10–15 minutes). This dose was selected by dose titration experiments to maintain MRI-visible glomeruli (data not shown). Urine protein concentration was determined by Bradford assay and creatinine by DetectX® from Arbor Assays (Ann Arbor, Michigan).

Ninety minutes after the injection of CF or saline, the rabbits received IM ketamine (80 mg/kg) and xylazine (10 mg/kg) followed by isoflurane. Both kidneys were cleared of blood by transcardiac perfusion. The left renal artery was clamped and 10% buffered formalin phosphate was perfused into the right kidney. Half of the left kidney was prepared for transmission electron microscopy (TEM) evaluation. The other half was immersion fixed

in formalin and embedded in paraffin. Kidney sections were stained with Periodic acid-Schiff and lotus lectin. The right kidney was stored in 2% glutaraldehyde/0.1 mol/L cacodylate for MRI.

MR Imaging Parameters: Kidneys were cut in half and put in 2% glutaraldehyde/0.1 mol/L cacodylate solution for imaging using a Bruker (Bruker, Co., Billerica, MA, USA) quadrature RF probe (inner diameter=30 mm). Imaging was performed on a Bruker 7T/30 MRI with Siemens software for acquisition and reconstruction (Siemens, Munich, Germany) and a gradient recalled echo (GRE) pulse sequence with the following parameters: TR:80, TE:20, 0.17 mm slice thickness, 29 mm field of view, 448*448 matrix, and a flip angle of 25°.

MRI data analysis: The images of each kidney were manually segmented and resolution (x, y, z) was increased by linear interpolation to 12.7 × 12.7 × 25 microns using Amira (FEL, Bordeaux, France) software. The medullary regions of the images were manually segmented. The kidney images were processed with MIPAR using an adaptive threshold. A 50% threshold value was used with a window size of 20 pixels. The glomerular images were analyzed with custom MATLAB, (The Mathworks, Natick, MA), scripts to obtain N_{glom} and V_{glom} . Within the images, there were some closely proximate glomeruli aligning along the same z-axis which appeared to be connected. The ratio of major to minor axis length for each glomerulus were used to compute the glomerular radius. aV_{glom} was measured by the number of voxels inside the cluster multiplied by the voxel dimensions. Apparent V_{glom} was then adjusted to account for the susceptibility artifact created by the CF in the glomerulus by multiplying it by the ratio of the average stereology-based value to the MRI-based value.

Transmission Electron Microscopy to confirm labeling: The tissue was processed for electron microscopy through the Advanced Microscopy Core at the University of Virginia. Briefly, the tissue was fixed overnight with 2.5% glutaraldehyde in 0.1M cacodylate buffer followed by three washes in 0.1M cacodylate buffer. The tissue was incubated for one hour in 2% osmium tetroxide in 0.1 M cacodylate buffer followed by two washes in cacodylate buffer then 10 minutes in distilled water. It was then dehydrated in serial grades of ethanol (30% to 100%) followed by 10 minutes in a 1:1 ethanol to propylene oxide solution. The samples were placed in a decreasing ratio of propylene oxide/epoxy resin (PO/EPON: 1:1-overnight, 1:2-3 hours, 1:4 overnight) followed by 24 hours in 100% EPON. The samples were embedded in fresh 100% epoxy resin and baked at 65 degrees. Sections were cut at 75 nm and placed on 200 copper grids. Each section was stained with 0.25% lead citrate and 2% uranyl acetate. The grids were carbon coated before imaging. Images were obtained on Transmission Electron Microscope, JEOL Model 1400 (Peabody, MA).

Cationic Ferritin Toxicity Studies:

To investigate the short- and long-term effects of CF, six week old rabbits received hydrocortisone sodium succinate followed by CF or saline. Each kit received lactated Ringer's solution (10 ml/kg) to mitigate transient weight loss (21) and was returned to its mother. At 24 hours, the rabbits were weighed and a blood sample was collected from the

marginal ear vein. Kits were monitored for 48 hours (CF, n=7; saline, n=4) or for four weeks (CF, n=4; saline, n=4) then euthanized. Intracardiac blood was collected and a complete blood count (CBC), iron level and comprehensive metabolic panel (CMP) were assessed. To further assess for systemic iron toxicity, the anion gap was calculated in mEq/L using the formula: anion gap=serum sodium-(serum chloride+serum bicarbonate). Kidneys, liver, lungs, and spleen were collected, weighed, formalin-fixed and paraffin embedded.

Histologic assessment of organs for toxicity—At 48 hours and four weeks after injection the kidney, liver, lung, and spleen were examined for changes in tissue microstructure and iron distribution. Structure was assessed with H&E and Periodic acid-Schiff (PAS) and iron was detected using Perls' Prussian blue stain as previously published (17).

Statistics

N_{glom} and apparent V_{glom} (aV_{glom}) were compared using the Mann Whitney U test with the AKI group compared to the healthy control group. aV_{glom} was separated into bins and t-tests were performed on each bin. In the toxicity studies, one way-ANOVA with multiple comparisons (Dunn's multiple comparison test) was used to assess blood parameters over time between the CF and saline groups. Two-way ANOVA was used to compare body weights over time. A two sample Kolmogorov-Smirnov test was used to test the distribution of aV_{glom} . Spearman rank correlation test was performed to assess associations. A two-sided significance level of 0.05 was set for all tests. Statistical analyses were performed using GraphPad Prism version 6.00 for Windows (GraphPad Software, La Jolla, California, USA).

RESULTS:

AKI studies:

We observed distinct kidney pathology at the time of AKI. Findings included a loss of brush border (Figure 1A-B) and proximal tubules (Figure 1C-D). There was no difference in serum creatinine between the groups (Figure 1E).

Following administration of gentamicin and indomethacin, the kits in the AKI group continued to gain weight. However, the final body weight of the AKI group at 6 weeks was 45% less than the control group (AKI: median: 750 (IQR: 725–885 g) versus control: 1370 (1330–1450 g), $p<0.01$, supplemental Figure S2A). The kidney weights of the AKI group were 32% less than in the control group (AKI: median: 9.3 g (IQR: 7.8–9.9) versus control: 13.6 g (12.9–16.9), $p<0.01$, supplemental Figure S2B). When the ratio of kidney weight to body weight was adjusted to account for sex differences, there was no difference between groups (AKI: median: 12 g/kg (IQR: 9.9–12.3) versus control: 9.9 g/kg (9.7–11.7), $p=0.28$, supplemental Figure S2C). Cortical volume measured by MRI was 46% lower in the AKI group as compared to the control group (AKI: 995 vs. control: 1868 mm³, $p<0.01$, supplemental Figure S2D). There was no difference in serum creatinine (Figure 1F) between the AKI (median: 0.6 mg/dl (IQR: 0.5–0.6)) and control (median: 0.6 mg/dl (0.53–0.6)) groups.

MRI Labeling studies:

The glomeruli in the control CF-labeled juvenile rabbit kidney appeared as dark spots in the cortex in MRI, consistent with CF accumulation in the glomerular basement membrane (GBM) (Figure 2A). A healthy, unlabeled rabbit exhibited no such spots (Figure 2B). Within the kidneys exposed to gentamicin and indomethacin, a circumferential region was detected in the CFE-MR images where glomeruli were absent or unlabeled (Figure 3A). The loss of glomerular labeling in CFE-MRI corresponded to an area of shrunken, immature glomeruli (Figure 3B) with reduced tubular mass (Figure 3C) observed in histologic sections.

The average number of glomeruli was 63% lower in the AKI group (AKI: median: 74,034 (IQR: 47,011–92,075) vs control: 198,722 (IQR: 148,221–232,028), $p < 0.01$, supplemental Figure S3A). Apparent V_{glom} was not different between the groups (AKI: median: $7.3 \times 10^{-4} \text{ mm}^3$ (IQR: 5.9–7.7) vs control: $6.2 \times 10^{-4} \text{ mm}^3$ (IQR: 5.6–8.3), $p = 0.69$, supplemental Figure S3C). There was not a significant correlation between cortical volume and N_{glom} (AKI: $r = 0.90$, $p = 0.08$, control: $r = 0.80$, $p = 0.13$). There was no correlation between N_{glom} and aV_{glom} in either group (supplemental Figure S3B). The distribution of aV_{glom} was also not different when the AKI group was compared to the controls (supplemental Figure S3D). There was no difference in urinary protein/creatinine between the AKI and control groups. Further details of each group are included in Table 1.

Confirmation of CF labeling by TEM:

As observed in other species (12-18), the CF traversed the fenestrated endothelium of the kidney and accumulated along the GBM. The location of the CF was confirmed in TEM (Figure 4A) and no CF was seen in non-injected control (Figure 4B). In contrast, CF labeling varied in the AKI group with a distinct subgroup of glomeruli where CF was visualized ultrastructurally in a patchy distribution that appeared to correspond to podocyte damage on the contralateral side of the GBM (Figure 4C-E). Additional TEM images are provided in supplemental Figure S4.

CF toxicity studies in juvenile rabbits:

A total of 19 rabbits were included in the toxicity studies and none died. Eleven were euthanized 48 hours after injection, CF (n=7) or saline (n=4). In the 48 hour group, body weights ranged from 1220–1400 g at the time of injection and 1260–1410 g at euthanasia. Eight animals were observed for 4 weeks after CF (n=4) or saline (n=4) injection.

Body weight: The CF group lost weight by 24 hours after injection (weight loss: 58 ± 54 grams, $p < 0.01$) but all animals regained this weight between 24 and 48 hours. There was no change in the body weights of the saline-injected group. There was no difference in body weights between CF group and controls at either 24 hours post-injection or at the end of the observation period (Figure 5A).

Gross and histologic organ assessment at 48 hrs and 4 wks: There was no difference in organ weights between the CF and saline groups, except for the livers. The CF group had ~20% heavier livers at 4 weeks (mean: CF: 65.7 ± 4.8 vs. saline: 53 ± 7.5 g,

$p < 0.001$), even after accounting for body weight: (CF: 30.9 ± 2.0 vs. saline: 25.4 ± 2.2 g/kg, $p < 0.001$) (Figure 5B).

A pathologist blindly examined histologic sections of the kidney, liver, lung, and spleen taken at 48 hours and 4 weeks after administration of CF or saline. Greater iron deposition was observed in the livers and spleens of the rabbits 48 hours after CF injection than in the saline-injected controls. Two of seven animals had iron in the glomeruli at 48 hours. There were no pathologic abnormalities noted in the CF group compared to the saline group.

Serum parameters at 48 hrs and 4 wks: Serum creatinine and blood urea nitrogen (BUN) were not different between the CF and saline groups at 48 hours (creatinine: CF 0.54 ± 0.05 vs saline 0.55 ± 0.06 mg/dL) or four weeks (creatinine: CF 0.67 ± 0.06 vs saline 0.70 ± 0.00 mg/dL). We assessed markers of iron toxicity including liver function parameters such as AST and ALT which were not different between the groups at any time point. There was no difference in anion gap between the CF and saline groups. There was a decrease in serum iron concentration in the CF group on the day 1 (CF: 109 ± 40.2 vs saline: 222 ± 26.0 U/L, $p = 0.006$), which returned to normal by day 2 (CF: 218 ± 40.3 vs saline: 226 ± 14.4 U/L, $p = 0.99$). The CF group exhibited a significant but transient increase in white blood cell (WBC) concentration for the two days following CF administration (day1: CF: 8.7 ± 1.9 vs saline: 5.3 ± 0.9 K/ μ L, $p = 0.003$; day2: CF: 11.3 ± 1.0 vs saline: 4.0 ± 1.2 K/ μ L, $p < 0.001$). The platelet concentration was lower in the CF group compared to the saline group on the day after CF administration (CF: 159 ± 21.9 vs. saline: 276 ± 90.7 K/ μ L, $p = 0.02$), but there was no difference by 48 hours (CF: 272 ± 53.5 vs. saline: 300 ± 98.5 K/ μ L, $p = 0.88$). There were no differences in any renal, liver or hematologic parameters four weeks after CF was given. Complete details of the serum parameters can be found in Table 2.

DISCUSSION:

Current clinical methods to evaluate kidney health, particularly serum creatinine, are inadequate, impairing early detection and potential prevention of AKI and CKD (23). This is especially true for preterm neonates, where the risk of CKD is impacted by iatrogenic exposures that result in aberrant nephrogenesis or nephron destruction during nephrotoxin-induced AKI (2, 4, 24-28). There is growing evidence that reduced nephron number at birth significantly increases the risk of CKD later in life (29-32). In this study, neonatal AKI rabbits undergoing active nephrogenesis were exposed to gentamicin and indomethacin to induce AKI. Based on CFE-MRI, those with AKI had 63% fewer nephrons (N_{glom}) 5 weeks after nephrotoxin exposure compared to the healthy controls. A circumferential region of injury was observed where nephrogenesis had been disrupted, clearly visible using CFE-MRI. Normal glomeruli occupied the regions superficial and deep relative to this injured area. Neither the extent nor the location of this damage were detectable by histologic assessment of the kidney biopsy, serum creatinine measurement, kidney-to-body weight ratio or cortical volume measurement of the kidney. In addition to the histologically visible, but MRI-invisible glomeruli, we believe that the reduced number of functioning nephrons was due to a combination of inhibited nephrogenesis and injury to preformed nephrons.

This work demonstrates that CFE-MRI is an effective tool to assess glomerular number in juvenile animals, providing a unique three-dimensional view of the kidney allowing detection of perfused, normal glomeruli. This provides evidence that glomeruli that may appear structurally normal on histology, may not be functionally normal (they cannot hold the CF on the GBM or may not be connected to tubules). Using TEM, we found that glomeruli in the unlabeled region on MRI had patchy or sporadic deposition of CF in the GBM, altered podocyte architecture with effacement, and reduced number of adjacent tubules. Proteinuria was not a significant finding in the AKI group despite evidence of podocyte effacement. Podocyte effacement was a localized phenomenon, limited to the regions where we also observed tubule loss. Without an intact glomerulo-tubular connection, we do not expect to detect proteinuria from these regions. The reduced labeling with CF in this localized circumferential area was also unlikely due to afferent arteriolar constriction because the glomeruli lacked erythrocytes following whole body perfusion. We conclude that CFE-MRI provides a functional measure of nephron number, which may serve as a useful biomarker of progression to CKD.

In this model of neonatal AKI, the visible histologic damage included tubular atrophy and loss. In addition to the layer of immature to relatively normal glomeruli arranged in a circumferential pattern, there was a normal-appearing subcapsular layer of glomeruli. These subcapsular glomeruli were labeled with CF, indicating that the removal of the AKI stimulus allowed for the resumption of nephrogenesis. This is an important observation, highlighting both the exquisite sensitivity of developing nephrons to toxins and the resilience of remaining nephron progenitors. However, the lack of replacement of the damaged nephrons is consistent with termination of nephrogenesis after the progenitor cell pool is depleted (33). A limitation of this study is the lack of a later time point to assess the evolution of the layer where there was tubular loss and glomerular damage. It is possible this area would become fibrotic, reabsorb, or that the tubules could undergo regeneration.

Although our follow-up period was relatively short, we hypothesized that reduced N_{glom} in the AKI cohort would lead to increased aV_{glom} . However, despite a large reduction in N_{glom} in the AKI cohort, there was no difference in aV_{glom} . The relationship between N_{glom} and V_{glom} is complex and incompletely understood. Factors that promote glomerular growth and later glomerulosclerosis include a reduction in N_{glom} , high protein, and high sodium diets. Growth hormone, insulin-like growth factor, androgens, glucocorticoids, and vasoactive hormones such as angiotensin and endothelin (34) can also promote glomerulomegaly and glomerulosclerosis. Genetic predisposition associated with race in humans and genetic background in animal models influence the hypertrophic response and the development of sclerosis. The timing of injury and age of the animal also modulate hypertrophy in response to nephron loss. There are several potential explanations for a similar glomerular size in our study including: 1) glomerular hypertrophy is not only a response to a low nephron number, but also a response to physiology stress and in this model the remaining nephrons are sufficient for the demands of the juvenile rabbit, 2) vasoconstriction from indomethacin may result in glomerular ischemia and prevent hypertrophy, 3) glomerular growth ceases with maturation, 4) the layer of glomeruli surrounded by fewer tubules are likely to be disconnected from tubules and these glomeruli are smaller due to a lack of filtration, and 5)

a lower dose and a single injection of CF was used for this study. This study emphasizes our limited understanding of the mechanisms of individual glomerular hypertrophy.

The principal advantage of CFE-MRI over traditional methods of glomerular enumeration is the potential for translation to humans. Although techniques such as the fractionator-disector and acid maceration methods to count glomeruli are robust (11, 35) they require destruction of the kidney. Recently, Denic et al (10) published their group's novel work on glomerular number with single nephron glomerular filtration rate in healthy adults estimated from total GFR, kidney biopsy and cortical volume of the kidney obtained from X-ray computed tomography (CT). Besides the risks of ionizing radiation and a renal biopsy, this may be a useful technique in the transplant evaluation process. However, it is not known if the correlation between cortical volume and nephron number is true in heterogenous models of kidney disease. CFE-MRI is the only nondestructive tool to assess glomerular number and size in the whole kidney, and it can be integrated with other types of MRI contrast to provide a comprehensive view of the kidney.

Significant work remains before CFE-MRI can be translated to humans, particularly the pediatric population. For CFE-MRI to be considered a screening tool, the expense and risk of the contrast and sedation would need to be low and balanced by a clear benefit and change in the natural course of CKD progression. Human administration of cationic protein-based agents from other species may raise safety concerns. For example, repeated doses of cationic bovine serum albumin are used in models of membranous glomerulopathy in mice (36) and rabbits (37). In an effort to translate CFE-MRI to humans, we continue to assess the short- and long-term effects of CF. Here, horse spleen-derived CF resulted a single day of weight loss, mild increased liver weight after 4 weeks, and a transiently increased white blood cell count, lower platelet count along with a decrease of serum iron concentration. The elevated WBC count and reduction in platelets may be a result of immunogenicity induced by a horse-derived product injected into the rabbit species as WBC demarginate and platelets may play a role in immune defenses (38). Further work is needed to determine the specific cause for these transient serologic abnormalities. Encouragingly, there was no evidence of iron toxicity, supported by normal liver function tests and a lack of histopathologic abnormalities. All serologic abnormalities had resolved by one week and remained absent at four weeks. Histologically there was no evidence of kidney, liver, lung or spleen injury and immune complexes were not visible on ultrastructural evaluation of the kidney.

Limitations of this study include the small numbers limiting further stratification. Our model was derived from an adult rodent model for AKI where the gentamicin dose was higher than the clinical dose of gentamicin used for neonates. However, the indomethacin dose is consistent with the dose used for neonates for closure of a patent ductus arteriosus. Lastly, the relationship between true individual glomerular volume and ("apparent") aV_{glom} measured by CFE-MRI is not yet completely understood. Therefore, changes in the measured distribution of aV_{glom} should be interpreted as relative changes between the AKI and control groups in this work.

In conclusion, indomethacin- and gentamicin-induced AKI during active nephrogenesis in rabbits results in a unique spatial distribution of kidney damage. CFE-MRI was used to

identify a unique circumferential lesion and assess the number of individual glomeruli, discriminating between healthy and injured glomeruli. We further demonstrated that CF does not cause toxicity in healthy neonatal rabbits. CFE-MRI provides a unique 3D view of the kidney, where novel information such as the long term effect on the kidney of nephrotoxin-induced AKI and number of perfused, intact glomeruli can be assessed. The translation of these metrics to patients, particularly in children, has the potential to assess nephron endowment and risk for future CKD and would allow for the development of therapeutics to halt or slow this progressive disease.

Supplementary Material

Refer to Web version on PubMed Central for supplementary material.

Acknowledgement:

Molecular Imaging Core (Rene “Jack” Roy), Advanced Microscopy Core, ACUC (Sanford Feldman, Gina Wimer, and Jeremy Gatesman).

Statement of financial support: The Hartwell Foundation, NIH/NIDDK: R01DK110622 and R01DK111861. This work used the Bruker ClinScan 7T MRI in the Molecular Imaging Core which was purchased with support from NIH grant 1S10RR019911-01 and is supported by the University of Virginia School of Medicine.

REFERENCES:

1. Hinchliffe SA, Sargent PH, Howard CV, Chan YF, van Velzen D 1991 Human intrauterine renal growth expressed in absolute number of glomeruli assessed by the disector method and Cavalieri principle. Laboratory investigation; a journal of technical methods and pathology 64:777–784. [PubMed: 2046329]
2. Rhone ET, Carmody JB, Swanson JR, Charlton JR 2013 Nephrotoxic Medication Exposure in Very Low Birth Weight Infants. The journal of maternal-fetal & neonatal medicine : the official journal of the European Association of Perinatal Medicine, the Federation of Asia and Oceania Perinatal Societies, the International Society of Perinatal Obstetricians.
3. Jetton JG, Boohaker LJ, Sethi SK, et al. 2017 Incidence and outcomes of neonatal acute kidney injury (AWAKEN): a multicentre, multinational, observational cohort study. The lancet child & adolescent health 1:184–194. [PubMed: 29732396]
4. Sutherland MR, Gubhaju L, Moore L, et al. 2011 Accelerated maturation and abnormal morphology in the preterm neonatal kidney. Journal of the American Society of Nephrology : JASN 22:1365–1374. [PubMed: 21636639]
5. Rodriguez MM, Gomez A, Abitbol C, Chandar J, Montane B, Zilleruelo G 2005 Comparative renal histomorphometry: a case study of oligonephropathy of prematurity. Pediatric nephrology (Berlin, Germany) 20:945–949.
6. Harer MW, Pope CF, Conaway MR, Charlton JR 2017 Follow-up of Acute kidney injury in Neonates during Childhood Years (FANCY): a prospective cohort study. Pediatric nephrology (Berlin, Germany) 32:1067–1076.
7. Hsu CW, Yamamoto KT, Henry RK, De Roos AJ, Flynn JT 2014 Prenatal Risk Factors for Childhood CKD. Journal of the American Society of Nephrology : JASN.
8. Rule AD, Amer H, Cornell LD, Taler SJ, et al. 2010 The association between age and nephrosclerosis on renal biopsy among healthy adults. Ann Intern Med 152:561–567. [PubMed: 20439574]
9. Doi K, Yuen PS, Eisner C, Hu X, Leelahavanichkul A, Schnermann J, Star RA 2009 Reduced production of creatinine limits its use as marker of kidney injury in sepsis. J Am Soc Nephrol 20:1217–1221. [PubMed: 19389851]

10. Denic A, Mathew J, Lerman LO, et al. 2017 Single-Nephron Glomerular Filtration Rate in Healthy Adults. *The New England journal of medicine* 376:2349–2357. [PubMed: 28614683]
11. Bertram JF 2013 Estimating glomerular number: why we do it and how. *Clinical and experimental pharmacology & physiology* 40:785–788. [PubMed: 24164176]
12. Baldelomar EJ, Charlton JR, Beeman SC, Bennett KM 2017 Measuring rat kidney glomerular number and size in vivo with MRI. *American journal of physiology.Renal physiology*:ajprenal.00399.02017.
13. Baldelomar EJ, Charlton JR, deRonde KA, Bennett KM In vivo measurement of kidney glomerular number and size in healthy and Os(+/-) mice using MRI. LID - 10.1152/ajprenal.00078.2019 [doi].
14. Baldelomar EJ, Charlton JR, Beeman SC, et al. 2015 Phenotyping by magnetic resonance imaging nondestructively measures glomerular number and volume distribution in mice with and without nephron reduction. *Kidney international*.
15. Beeman SC, Cullen-McEwen LA, Puelles VG, et al. 2014 MRI-based glomerular morphology and pathology in whole human kidneys. *American journal of physiology.Renal physiology* 306:F1381–1390. [PubMed: 24647716]
16. Beeman SC, Zhang M, Gubhaju L, et al. 2011 Measuring glomerular number and size in perfused kidneys using MRI. *American journal of physiology.Renal physiology* 300:F1454–1457. [PubMed: 21411479]
17. Bennett KM, Zhou H, Sumner JP, et al. 2008 MRI of the basement membrane using charged nanoparticles as contrast agents. *Magnetic resonance in medicine : official journal of the Society of Magnetic Resonance in Medicine / Society of Magnetic Resonance in Medicine* 60:564–574.
18. Heilmann M, Neudecker S, Wolf I, et al. 2012 Quantification of glomerular number and size distribution in normal rat kidneys using magnetic resonance imaging. *Nephrology, dialysis, transplantation : official publication of the European Dialysis and Transplant Association - European Renal Association* 27:100–107.
19. Kazimierzczak J 1963 Histochemical Study of Oxidative Enzymes in Rabbit Kidney before and After Birth. *Acta Anatomica* 55:352–369. [PubMed: 14156454]
20. Hosaka EM, Santos OF, Seguro AC, Vattimo MF 2004 Effect of cyclooxygenase inhibitors on gentamicin-induced nephrotoxicity in rats. *Brazilian journal of medical and biological research = Revista brasileira de pesquisas medicas e biologicas* 37:979–985. [PubMed: 15264004]
21. Charlton JR, Pearl VM, Denotti AR, et al. 2016 Biocompatibility of ferritin-based nanoparticles as targeted MRI contrast agents. *Nanomedicine : nanotechnology, biology, and medicine*.
22. Danon D, Goldstein L, Marikovsky Y, Skutelsky E 1972 Use of cationized ferritin as a label of negative charges on cell surfaces. *Journal of ultrastructure research* 38:500–510. [PubMed: 4111070]
23. Moran Sm Fau - Myers BD, Myers BD Course of acute renal failure studied by a model of creatinine kinetics.
24. Gubhaju L, Sutherland MR, Yoder BA, Zulli A, Bertram JF, Black MJ 2009 Is nephrogenesis affected by preterm birth? Studies in a non-human primate model. *American journal of physiology.Renal physiology* 297:F1668–F1677. [PubMed: 19759270]
25. Popescu CR, Sutherland MR, Cloutier A, et al. AM 2013 Hyperoxia exposure impairs nephrogenesis in the neonatal rat: role of HIF-1alpha. *PLoS one* 8:e82421. [PubMed: 24358181]
26. Kent AL, Brown L, Broom M, Broomfield A, Dahlstrom JE 2012 Increased urinary podocytes following indomethacin suggests drug-induced glomerular injury. *Pediatric nephrology (Berlin, Germany)* 27:1111–1117.
27. Kent AL, Koina ME, Gubhaju L, et al. 2014 Indomethacin administered early in the postnatal period results in reduced glomerular number in the adult rat. *American journal of physiology.Renal physiology* 307:F1105–1110. [PubMed: 25186294]
28. Gilbert T, Lelievre-Pegorier M, Merlet-Benichou C 1991 Long-term effects of mild oligonephronia induced in utero by gentamicin in the rat. *Pediatric research* 30:450–456. [PubMed: 1754301]
29. Brenner BM, Garcia DL, Anderson S 1988 Glomeruli and blood pressure. Less of one, more the other? *American journal of hypertension* 1:335–347. [PubMed: 3063284]
30. Brenner BM, Mackenzie HS 1997 Nephron mass as a risk factor for progression of renal disease. *Kidney international.Supplement* 63:S124–127. [PubMed: 9407439]

31. Kanzaki G, Puelles VG, Cullen-McEwen LA, et al. 2017 New insights on glomerular hyperfiltration: a Japanese autopsy study. *JCI insight* 2:10.1172/jci.insight.94334.
32. Keller G, Zimmer G, Mall G, Ritz E, Amann K 2003 Nephron number in patients with primary hypertension. *The New England journal of medicine* 348:101–108. [PubMed: 12519920]
33. Hartman HA, Lai HL, Patterson LT 2007 Cessation of renal morphogenesis in mice. *Developmental biology* 310:379–387. [PubMed: 17826763]
34. Fogo A, Ichikawa I 1991 Evidence for a pathogenic linkage between glomerular hypertrophy and sclerosis. *American Journal of Kidney Diseases : The Official Journal of the National Kidney Foundation* 17:666–669. [PubMed: 2042646]
35. Bertram JF, Cullen-McEwen LA, Egan GF, et al. 2014 Why and how we determine nephron number. *Pediatric nephrology (Berlin, Germany)* 29:575–580.
36. Chen JS, Chen A, Chang LC, et al. 2004 Mouse model of membranous nephropathy induced by cationic bovine serum albumin: antigen dose-response relations and strain differences. *Nephrology, dialysis, transplantation : official publication of the European Dialysis and Transplant Association - European Renal Association* 19:2721–2728.
37. Border WA, Ward HJ, Kamil ES, Cohen AH 1982 Induction of membranous nephropathy in rabbits by administration of an exogenous cationic antigen. *The Journal of clinical investigation* 69:451–461. [PubMed: 7056856]
38. Cloutier N, Allaey I, Marcoux G, et al. 2018 Platelets release pathogenic serotonin and return to circulation after immune complex-mediated sequestration. *Proceedings of the National Academy of Sciences of the United States of America* 115:E1550–E1559. [PubMed: 29386381]

Impact questions:

- Nephrotoxin exposure during nephrogenesis results in fewer glomeruli and glomerular maldevelopment.
- Using CFE-MRI, we detected a circumferential pattern of cortical nephron loss in a location and distribution that is less discernable using traditional techniques.
- Nephrotoxic medications, such as indomethacin and gentamicin, are commonly used in the neonatal intensive care unit and can contribute to the development of adult chronic kidney disease (CKD). It is critical to develop better tools to diagnose CKD in its earliest stages, to enable new therapies to halt or slow its progression. CFE-MRI may eventually be translated to provide a nondestructive measure of nephron loss in humans.

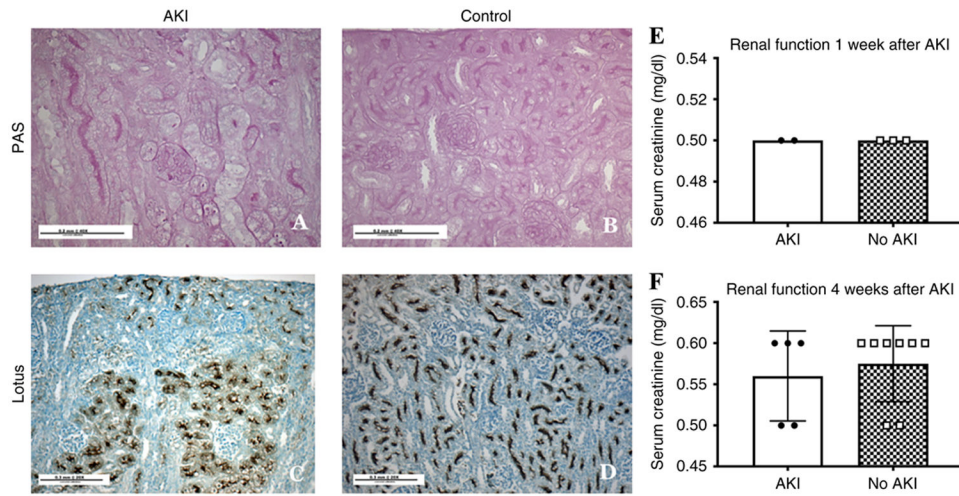


Figure 1. Histology and renal function at the time of acute kidney injury.

Histology sections of a rabbit kidney just following gentamicin and indomethacin (AKI: panels A and C) compared to a control that did not receive gentamicin and indomethacin. Most notable is the lack of proximal tubules (C) in the AKI model. There was no difference in renal function measured by serum creatinine 2 weeks after the induction of AKI (E) and at 6 weeks of age following AKI (F).

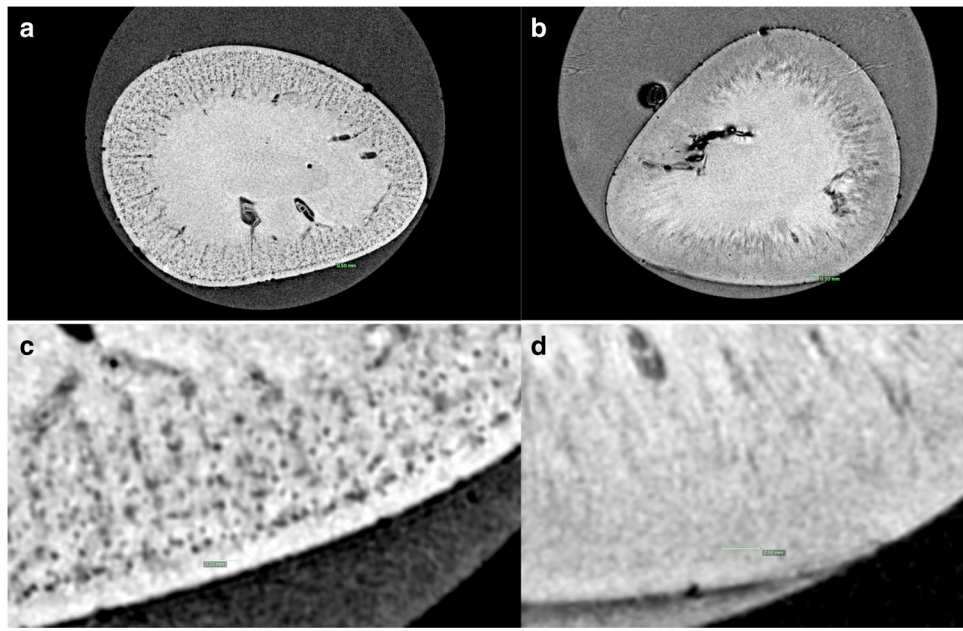


Figure 2. Representative MR image of cationic ferritin enhanced MRI (A) and control without cationic ferritin (B).

The systemically administered cationic ferritin transiently binds to the glomerular basement membrane and allows each glomerulus to be MRI detectable (a). However, even at high field strength there is not enough contrast between the glomeruli and surrounding vasculature and tubules to detect the glomeruli without an exogenous contrast agent (b). Distinct black dots can be seen in greater detail at high magnification (c) but no glomeruli are visible without the contrast (d). Green scale bar represents 0.5 mm.

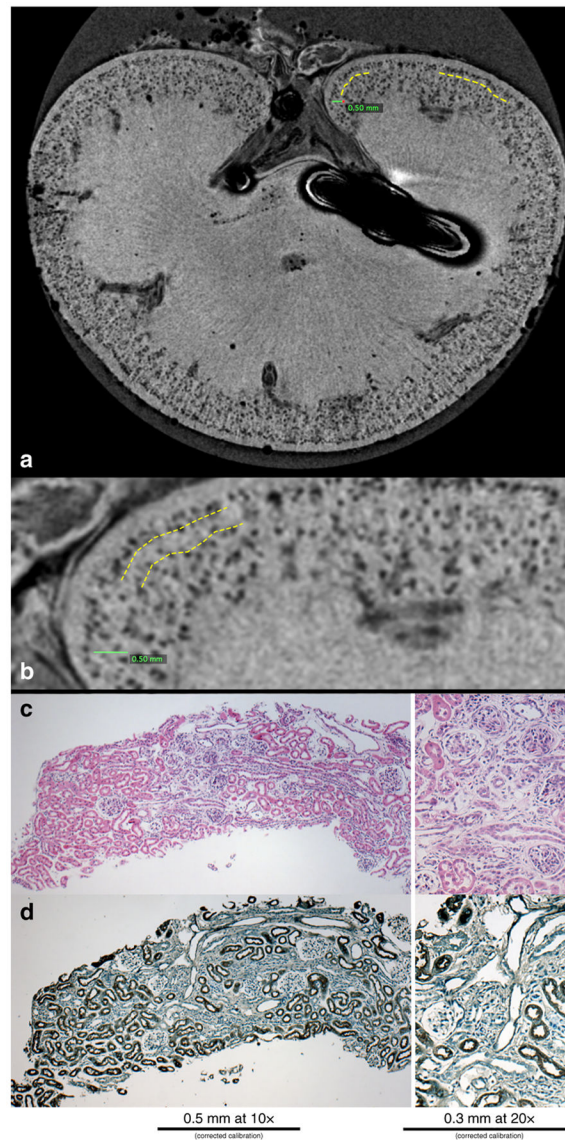


Figure 3. Nephrotoxin-induced AKI during nephrogenesis results in a circumferential layer of glomeruli where cationic ferritin is heterogeneously detected.

A representative MR image from a kidney from the AKI group where glomerular drop out is outlined in the yellow dotted lines (a). This area is magnified in (b) where the yellow dotted lines outline the boundaries of the area with glomerular drop out and there are glomeruli just under the capsule that are normal appearing and label with CF. Histologically this area has shrunken, immature glomeruli by PAS (c), with a lack of surrounding proximal tubules by lotus (d).

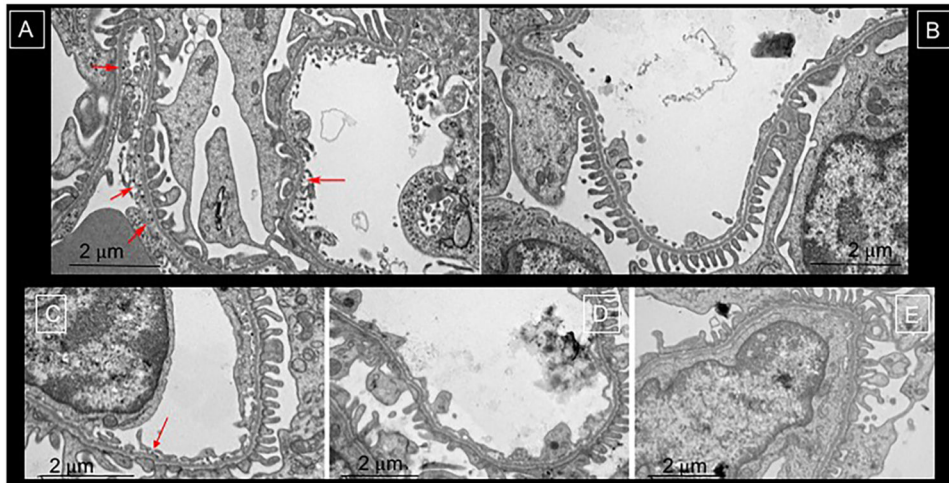


Figure 4. Transmission Electron Microscopy to validate cationic ferritin distribution in healthy (A), saline-injected controls (B) and those with AKI (C-E).

In panel A, the red arrows highlight the cationic ferritin traversing the endothelium and in the glomerular basement membrane. Whereas, there is no such labelling in panel B where the rabbit was injected with saline. In the rabbits exposed to AKI (C-E) the glomeruli in the damaged circumferential layer had heterogeneous and reduced labeling of CF in the glomerular basement membrane in C (red arrow indications CF deposition) and no CF in panels D and E. There was often podocyte effacement in these areas of reduced or lack of CF deposition.

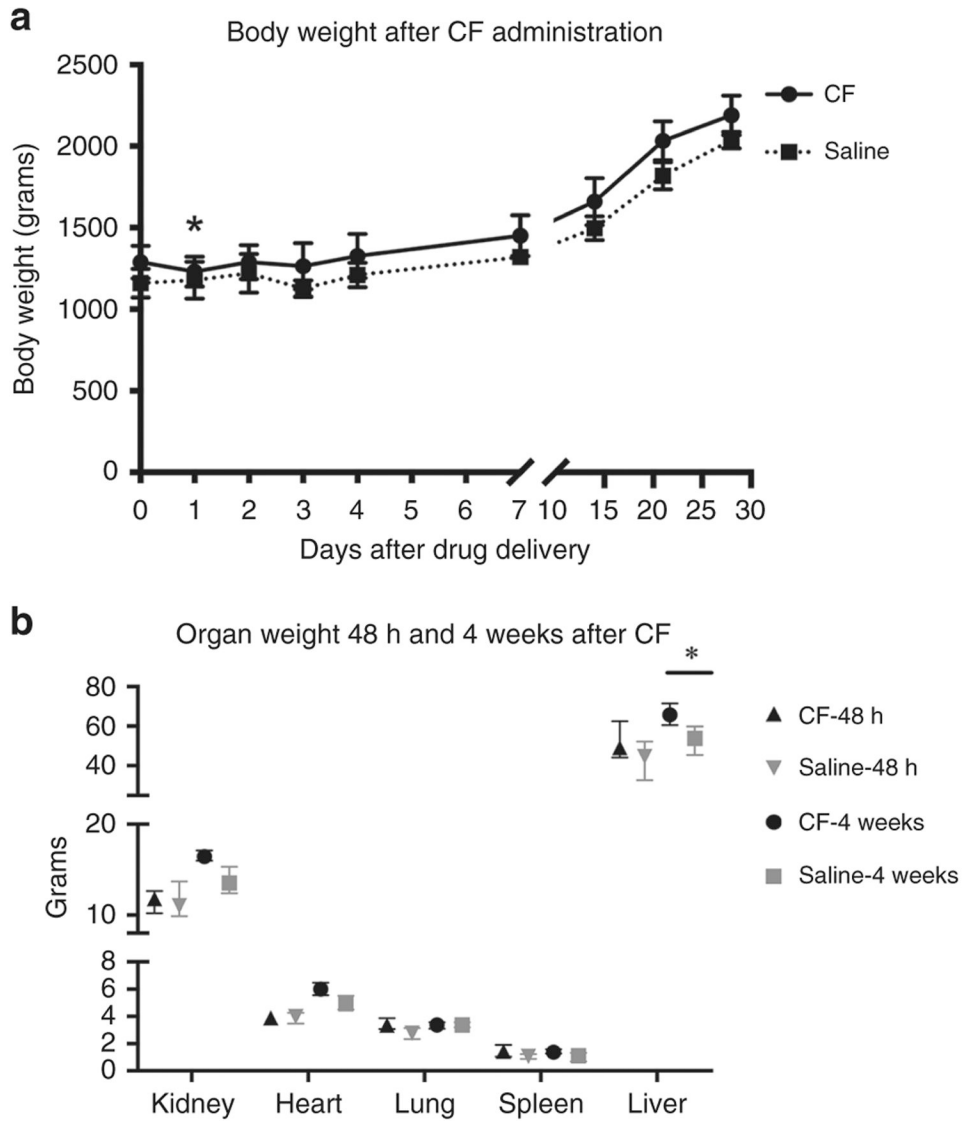


Figure 5. Body and organ weight after CF administration in healthy rabbits. Many of the rabbits that received CF at 6 weeks, initially lost weight in the first 24-48 hours ($p < 0.01$), but then gained weight by day 2 after CF (panel A). At the end of the observation period there was no difference in the body weights of the rabbits that received CF as compared to those who received saline. Organ weight was assessed at 2 time points: 48 hours and 4 weeks after CF. There was no difference in organ weight either by raw measurements (panel B) or when adjusted to body weight, with the exception of a heavier liver weight 4 weeks after CF was administered.

Table 1:

Glomerular number and volume by MRI and stereology.

	Body weight (kg)	Total kidney weight (g)	KW(g)/BW(kg)	Cortical volume (mm ³)	MRI N _{glom}	MRI aV _{glom} (x 10 ⁻⁴ , mm ³)
AKI	0.70	8.6	12.2	937	74034	7.77
	0.86	10.3	12.0	1175	97334	7.72
	0.75	9.3	12.4	1024	86815	5.76
	0.91	9.6	10.6	995	53614	7.30
	0.75	6.9	9.2	751	40407	6.01
controls	1.31	12.7	9.7	1717	167017	6.16
	1.40	16.1	11.5	2137	262636	7.21
	1.50	17.7	11.8	2179	201419	5.86
	1.35	13.1	9.7	1868	198722	5.36
	1.37	13.6	9.9	1748	129425	9.35

Table 2.

Systemic surveillance of CF toxicity

days after injection	CF			saline			CF			saline		
	mean	SD	number	mean	SD	number	mean	SD	number	mean	SD	number
creatinine (mg/dl)												
0	0.52	0.06	10	0.58	0.04	6	10.1	2.6	10	10.8	2.8	6
1	0.57	0.05	7	0.55	0.06	4	13.3	2.9	7	10.0	1.2	4
2	0.54	0.05	7	0.55	0.06	4	10.9	1.7	7	10.0	0.8	4
7	0.55	0.06	4	0.60	0.00	3	10.0	0.0	4	11.7	2.5	3
28	0.67	0.06	3	0.70	0.00	3	12.3	1.2	3	10.0	1.0	3
ALT (U/L)												
0	32.9	31.3	10	20.3	7.9	6	30.6	7.3	10	27.5	7.5	6
1	17.1	14.5	7	13.3	4.0	4	35.1	12.1	7	31.5	5.1	4
2	19.9	13.4	7	26.3	13.2	4	23.6	4.9	7	31.3	6.3	4
7	17.0	5.8	4	20.7	3.5	3	19.5	2.4	4	22.3	8.6	3
28	23.7	10.8	3	24.0	9.5	3	24.7	2.5	3	33.3	9.5	3
iron (U/L)												
0	191.8	40.2	10	211.8	26.0	6	16.1	2.2	10	16.2	1.6	6
1	109.3	84.0	7	222.5	13.0	4	16.3	1.8	7	15.3	1.5	4
2	218.0	40.3	7	226.5	14.4	4	13.1	2.3	7	12.0	2.9	4
7	242.3	47.6	4	242.3	26.4	3	18.0	2.7	4	14.3	4.9	3
28	217.7	14.0	3	178.7	51.4	3	12.0	4.4	3	13.0	1.0	3
white blood cell (k/mcl)												
0	5.9	0.9	10	6.5	1.4	6	189.9	44.6	10	238.7	32.9	6
1	8.8	1.9	7	5.4	0.9	3	159.3	21.9	7	276.0	90.7	3
2	11.4	1.0	6	4.0	1.2	4	272.0	53.5	6	300.5	98.5	4
7	6.8	0.8	4	5.8	2.0	3	233.8	79.9	4	237.7	30.9	3
28	2.3	1.5	3	3.6	1.8	3	238.0	37.2	3	261.7	66.5	3

*** The bolded values were statistically significantly different, iron day 1, p=0.001; WBC day 1, p=0.003, day 2, p<0.001; platelets day 1, p=0.02